

Multilayer relaxation and search for ferromagnetic order at the (100) surface of bulk paramagnetic vanadium

D. Lacina, J. Yang, and J. L. Erskine

Department of Physics, The University of Texas at Austin, Austin, Texas 78712, USA

(Received 4 April 2006; revised manuscript received 22 February 2007; published 17 May 2007)

Low-energy-electron-diffraction (LEED) intensity measurements and multiple-scattering analysis for V(100), supported by accurate characterization of surface impurity concentrations based on Auger-electron spectroscopy, are used to obtain a meaningful extrapolation of the first-layer relaxation to the clean surface value: $d_{12}=1.36\pm 0.05$ Å, corresponding to $\Delta_{12}=-10\%\pm 3\%$ relative to the bulk value $d_0=1.514$ Å. A high-sensitivity probe for surface magnetism based on magneto-optic Kerr effect polarimetry using the cleanest surfaces achieved in the LEED experiment ($\sim 5\%$ C) yields a (sensitivity limited) null result with an estimated upper limit of $0.05 \mu_B/\text{surface atom}$. These results are discussed within the framework of related experiments and in relation to the predictive accuracy of *ab initio* calculations that explore the surface structure and magnetism of V(100) both of which are sensitive to different approximations for the exchange-correlation potential in density-functional theory.

DOI: [10.1103/PhysRevB.75.195423](https://doi.org/10.1103/PhysRevB.75.195423)

PACS number(s): 61.14.Hg, 61.66.Bi, 75.70.Rf, 73.20.-r

I. INTRODUCTION

Vanadium is a high susceptibility paramagnet that can exhibit ferromagnetic behavior under certain conditions, notably in thin films coupled to a ferromagnetic substrate.¹⁻⁵ This feature, along with the close relationship between the occurrence of ferromagnetism, atomic coordination, and the relevant surface or bulk lattice parameter, has resulted in extensive use of the (100) surface of vanadium as a venue for testing the predictive accuracy of *ab initio* calculations.⁶⁻¹³ A prior (1986) experiment¹⁴ based on electron-capture spectroscopy, which reported observation of ferromagnetic order at the V(100) surface, has helped sustain interest in resolving significant differences¹¹ in the multilayer relaxation and magnetic properties of V(100) predicted by two principle classes of theoretical approaches: pseudopotential calculations vs all-electron calculations. Table I summarizes some of the recent values of surface magnetic moments and multilayer relaxation for V(100) predicted based on various *ab initio* approaches.

Two general trends emerge from Table I. One trend is the prediction of ferromagnetic ordering at the surface by pseudopotential methods and the absence of magnetism predicted by the all-electron methods.⁶⁻¹¹ This issue has been reviewed in relation to results for V(100) by Robles *et al.*¹¹ and Batyrev *et al.*⁸ The central experimental issue relative to the first trend noted from Table I is the validity of the electron-capture experiment:¹⁴ Is the surface layer of V(100) ferromagnetic?

The second trend apparent from Table I is the tendency of all *ab initio* calculations to predict first-layer relaxations (Δ_{12}) of V(100) that are significantly larger than the experimental values^{13,15} determined by low-energy-electron-diffraction (LEED) crystallography. This trend is not unique to V(100).

Ten years ago, Feibelman^{16,17} noted systematic discrepancies between first-layer surface relaxations predicted by first-principles calculations and corresponding results obtained from surface crystallography. The discrepancies, which ex-

ceeded the accepted accuracy of both the experiments and the calculations, were observed to be particularly apparent for reactive transition-metal surfaces where results differing by a factor of 2 were not uncommon.¹⁸⁻²¹ This dilemma is troubling because density-functional calculations provide an important tool for seeking detailed and comprehensive understanding of a broad range of surface phenomena ranging from the electronic properties of surfaces, including chemical bonding and reactivity, to surface magnetism. The cornerstone for understanding the electronic, chemical, and magnetic behaviors of surfaces is an accurate atomic structure model of the surface. If *ab initio* calculations based on the local-density approximation are incapable of accurately predicting the equilibrium positions of surface atoms (a ground-state property that can presumably be determined experimentally), one might justifiably question the predictive accuracy of *ab initio* calculations when applied to other surface phenomena such as the occurrence of surface magnetism.

Efforts to identify a universal basis for the systematic discrepancy between calculated and measured surface relaxations have had limited success. In the specific case of V(100), significant differences in the calculated values of Δ_{12} (Table I) have been attributed to the details of the computational method¹³ applied to surfaces, but the same methods yield essentially identical values for the bulk lattice constants of V ($d_{\text{th}}=2.99$ Å) when the same generalized gradient approximation (GGA) is utilized to describe the exchange-correlation potential. The theoretically predicted value d_{th} is in good agreement with the experimental value $d_0=3.03$ Å for bulk V.

Corresponding recent efforts, which have carefully evaluated certain elements of surface crystallography based on LEED intensity versus voltage (*I-V*) measurements, have also failed to identify a universal source of systematic error.¹⁸⁻²¹ For example, the following issues have recently been addressed by experiments: (1) the effects on structure determination based on LEED arising from surface roughness has been evaluated and shown to be negligible (under conditions achieved in typical experiments) based on system-

TABLE I. Recent values of calculated and measured first-layer (Δ_{12}) and second-layer (Δ_{23}) relaxations of V(100). Δ_{ij} are presented in terms of percent change of bulk lattice spacing $d = 1.515 \text{ \AA}$. Magnetic moment (right column) in Bohr magnetons corresponds to first-layer spin polarization. The experimental lattice constant was used in the calculations of surface magnetization by Robles *et al.* (Ref. 11).

		Δ_{12} (%)	Δ_{23} (%)	μ_B (surface)
Experiments				
Jensen <i>et al.</i> (Ref. 15)		-6.9	+1.0	
Bergermayer <i>et al.</i> (Ref. 13)		-8.6	+1.3	
Calculations				
Billmayer <i>et al.</i> (Ref. 9)	(7 layer)	-10.4		0.04
	(15 layer)	-11.1	+0.7	0.00
Batyrev <i>et al.</i> (Ref. 8)		-12.5	+0.9	0.75
Bergermayer <i>et al.</i> (Ref. 13)	VASP/US	-15.7	+0.47	
	VASP/PAW	-13.3	+0.67	
	FLEUR	-11.1	+0.67	
Robles <i>et al.</i> (Ref. 11)	GGA/LMH	Experimental		0.66
	GGA/PW	lattice		0.25
	LSDA(AE/PP)	constant		0.00

atic measurements on stepped surfaces;¹⁹ (2) modern multiple-scattering codes have been shown to be robust by comparing calculated LEED intensity spectra obtained from the Van Hove–Tong (renormalized forward scattering) and Xerox (matrix inversion) codes using identical input parameters;^{18,22} (3) convergence tests that evaluate the accuracy of structure determination resulting from truncating the cumulative energy range of an I - V data set (and based on different r -factor criteria) have shown that two of the most commonly used r factors (Pendry r_p and Zanazzi-Jona r_{zj}) yield compatible results provided the data set is adequate (cumulative range of all nondegenerate beams is greater than 1000 eV) (Ref. 18) and the r factors are suitably low.

Some of the recent LEED studies have also considered the compatibility of data sets measured by independent groups using separately prepared samples and different methodologies.^{18–20} In two cases, Rh(100) (Ref. 18) and W(110) (Ref. 19) two such data sets were found to be in excellent agreement, and in a third case, Ti(0001),²⁰ the differences could be attributed to sample contamination effects. These consistency evaluation exercises can be considered an extension of the 1980 international LEED project^{23,24} carried out on Cu(100) that was designed to assess the intrinsic accuracy of LEED I - V methodology. All evidence to date suggests that LEED methodology is robust.

One possible source of structure-determination inaccuracy has been identified in surface crystallography experiments. This inaccuracy is related to the effects of surface hydrogen. The problem arises because the predominate residual gas in ultrahigh vacuum systems (base pressure in the 10^{-11} Torr

range) is H_2 . Hydrogen dissociatively adsorbs on transition-metal surfaces, and atomic hydrogen cannot be detected by Auger-electron spectroscopy (AES), the most common probe of surface cleanliness. Chemical impurities adsorbed on a surface increase the bonding coordination of the surface atoms, which generally results in a reduction of the local first-layer relaxation. Low concentrations (below 10%) of disordered impurities on an otherwise well-ordered single-crystal metal surface results in lower reliability factors (r factors) in LEED analysis and smaller values of the actual as well as the determined top-layer relaxation. The difference between the clean surface relaxation determined by LEED analysis and the corresponding result from a slightly contaminated surface (concentration of <10%) scales linearly with impurity concentration similar to other parameters, such as the work function, that are strongly influenced by charge-transfer effects associated with surface chemical bonding.²⁵ A significant reduction of the clean-surface relaxation resulting from undetected surface hydrogen or other impurities at concentrations below the AES sensitivity limit could account for some of the disagreements between calculated and measured structural parameters. This effect is especially important in highly reactive metal surfaces [for example, Ti(0001)] and has been shown to account for inaccuracies in prior evaluations of surface relaxation²⁰ of that surface.

The present paper describes experiments that address the surface structure and magnetism of V(100) from the viewpoint of issues outlined in this Introduction. The experiments strive to answer two key questions that are relevant to predictions based on *ab initio* calculations for V(100): (1) Is the surface magnetic and (2) what is the first-layer relaxation? Because it has not been possible to prepare a perfectly clean and perfectly ordered V(100) surface, these two questions (and answers) must be modified to reflect experimental limitations. However, the results presented still provide a meaningful basis for judging the predictive capabilities of various forms of *ab initio* calculations that have been extensively applied to V(100).

II. EXPERIMENTAL PROCEDURES

The surface structure measurements were carried out using a UHV instrument that incorporates LEED, AES, electron-energy-loss spectroscopy (EELS), and ultraviolet photoemission spectroscopy (UPS) capabilities. The LEED intensity versus voltage (I - V) spectra were measured by frame-grabbing instrumentation interfaced to an SIT camera. The methodology, including extensive experiments required to characterize the effects of adsorbed hydrogen on Ti(0001) at the base pressure (directly probed by EELS which measures vibrational excitations and indirectly by UPS as changes in work function), has been described, in detail, in prior publications.^{18–20} The instrument base pressure with liquid-nitrogen-cooled Ti sublimation pumping ($<5 \times 10^{-11}$ Torr) is adequately low to reduce undesired H and CO surface contaminations during the (40 min) periods required to log a set of I - V spectra to below 0.01–0.02 ML (monolayer). The magneto-optic Kerr effect studies were carried out in a different UHV instrument (with similar low base

pressure) that also incorporates LEED and AES surface probes into a high-sensitivity magneto-optic Kerr effect polarimeter. This instrument was previously used in an experiment that probed for ferromagnetic ordering of $p(1 \times 1)$ V on Ag(100) (Ref. 26) and has also been described in prior publications.²⁷

Sample preparation and characterization of V(100) presented significant challenges, as noted in prior publications.^{13,15,28–34} The first attempt to determine the surface structure of V(100) (Ref. 28) was carried out on a (5×1) reconstructed surface which was believed to be clean. Recent studies of V(100) that combine high-resolution AES and scanning tunneling microscopy have shown that the (5×1) reconstruction is stabilized by low concentrations of oxygen (~ 0.2 ML).^{15,33} When a low concentration of carbon is also present, it is possible to detect spatial inhomogeneity of carbon and oxygen contaminations, which manifests a superposition of $c(2 \times 2)$ and (5×1) diffraction patterns by moving the primary LEED beam across the surface. The recent studies of adsorbates on V(100), including careful studies of hydrogen adsorption and desorption kinetics³³ and the bulk/surface diffusion of C and O,³⁰ provide a useful body of knowledge for preparing and characterizing a “clean” V(100) surface.

The V(100) sample used in experiments described in this paper was cut from an oriented single-crystal boule (99.9 + % purity). The 12 mm diam \times 2 mm thick sample was spark cut by an electric discharge milling machine using a moving wire electrode. The sample was aligned using x-ray Laue back-diffraction techniques assisted by ORIENT EXPRESS software.³⁵ After mechanical polishing using alumina and diamond abrasives to 0.25 μm particle size, the (100) crystal axis was determined to be aligned with the surface normal to an accuracy exceeding $\pm 0.5^\circ$. The surface-step density and roughness associated with this orientation accuracy is below the detection limit of conventional LEED optics (for observing spot splitting) and far below the step density threshold shown to result in structure determination errors based on LEED intensity measurements.¹⁹

The sample was mounted on a manipulator at the tip of a UHV liquid-nitrogen dewar that permitted precise orthogonal two-axis rotation about the crystal face. This orientation capability was used to align the (100) crystallographic axis parallel with the incident electron beam from the LEED optics. The sample could be heated by an electron beam from the back and could be cooled to 150 K. A Chromel-Alumel thermocouple attached to the crystal (in addition to a handheld pyrometer with an infrared filter) was used to measure sample temperature.

Extensive *in situ* sample cleaning and annealing was required to achieve a clean and well-ordered surface. The initial sample conditioning consisted of repeated cycles of ion sputtering at glancing incidence (ion gun operating at 15 mA emission, 2 kV, and 1×10^{-4} Torr Ne yielding $\sim 10 \mu\text{A}$ current at the sample) followed by high-temperature annealing. During the initial cleaning cycles, AES detected near-surface contaminants of phosphorous, sulfur, carbon, and oxygen. Surface phosphorous and sulfur were depleted after about 80 h of repeated sputtering and annealing to 1200 K.

The final stage of sample cleaning requires removal of near-surface carbon and oxygen. Carbon segregation from the bulk to the surface occurs at 600 K and carbon surface diffusion occurs at ~ 750 K. Oxygen segregation to the surface occurs over the range of 600–950 K, but oxygen absorbs into the bulk at higher temperature.³⁰ The combination of bulk and surface diffusion of C and O and the high sticking probability of O and CO (and H) is the source of difficulty in obtaining a clean V(100) crystal surface. The problem is exacerbated by the near overlap of the primary oxygen AES peak (512 eV) with a prominent vanadium peak (510 eV). The peaks can be resolved by using a low ($< 2 V_{p-p}$) modulation voltage and slow energy scan rates when conducting AES. The following AES calibration results^{13,30} were used to judge the concentration of C and O impurities on V(100): 1 ML C corresponds to a $C_{272}/V_{473} dN/dE$ peak ratio of 0.10 and 1 ML of O corresponds to a $O_{510}/V_{473} dN/dE$ peak ratio of 0.066 and a $O_{492}/V_{473} dN/dE$ peak ratio of 0.022.

Final sample conditioning required over 1000 h of sputtering, annealing, and flashing cycles following a procedure similar to that described by Jensen *et al.*¹⁵ The primary difference in our procedure was that neon was used as the sputtering gas. This permitted maintaining the titanium sublimation pump cryoshroud at 77 K (filled with LN_2) and permitted the LEED experiments to be carried out in the 8×10^{-11} Torr range. The sputtering, annealing (600–700 K), and flashing (to 1000 K) finally resulted in a well-ordered (1×1) surface with O, P, and S contaminations below the AES sensitivity limit (0.01 ML). Continuous use of the LN_2 -cooled titanium sublimation pump during the final stages of sample conditioning and during measurements ensured CO and H partial pressures below 5×10^{-11} Torr and reduced the effects of surface contamination by residual gas to below 1%–2% of a ML during the 40 min period required to log LEED spectra.

The highest quality clean V(100) surface achieved in our experiments yielded AES spectra that indicated about 5% C ($C_{272}/V_{473} \cong .005$) and no other impurities at the sensitivity limit which was judged to be 1% for oxygen. The residual surface C was judged to originate from bulk diffusion during final annealing required to obtain a well-ordered surface. Additional C concentration and detectable O contamination were always observed after a long high-sensitivity AES scan (30 min) or after logging LEED spectra (40 min) that is attributed to CO production from the tungsten filaments. The total surface contamination determined by AES after a complete set of LEED *IV* spectra had been taken was typically 6%–8% and mostly C. The magneto-optical Kerr effect (MOKE) measurements were carried out at the lowest limit of C contamination ($\leq 5\%$).

III. LEED DATA AND ANALYSIS

LEED *I-V* data sets were acquired after symmetrizing conjugate (symmetry degenerate) beam intensities in the usual manner: The orientation of the sample was adjusted until all conjugate beams yielded the same intensity. This process ensures normal incidence of the electron beam. Pen-

dry r -factor analysis was used to characterize the internal consistency of the individual beams with their averages. The four-beam cumulative energy range is 1100–1200 eV, depending on the specific data set, which is adequate, based on prior studies¹⁹ to achieve convergence leading to an accurate structure determination. Typical r_p values for conjugate beam-averaged beam comparison of unsmoothed I - V spectra are (10) beams (450 eV range) $r_p \sim 0.19$, (11) beams (350 eV range) $r_p \sim 0.038$, (20) beams (300 eV range) $r_p \sim 0.09$, and (21) beams (200 eV range) $r_p \sim 0.085$.

Continuing the tradition of our prior LEED publications,^{18–20} we evaluated the compatibility of our data with relevant prior work (where I - V spectra were available) by digitizing the results of Jensen *et al.*¹⁵ and conducting r -factor comparison of the averaged inequivalent beams with our unprocessed I - V spectra. Pendry r -factors comparing one of our room temperature I - V data sets (~ 1000 eV range for nondegenerate beams) with the published data set Jensen *et al.*¹⁵ yielded an averaged value $r_p \sim 0.45$. The agreement is not equivalent to the excellent agreement achieved in corresponding comparisons for Rh(100) (Ref. 18) and W(100).¹⁹ For example, in our comparison of an independently measured Rh(100) data set, we obtained Zanazzi-Jona r factors in the range $r_{zj} \sim 0.04$ – 0.06 ; for W(100), a similar comparison yielded Pendry r factors $r_p \sim 0.202$. Some of the (relatively large) differences between our (unsmoothed) I - V data and the data of Jensen *et al.* can be attributed to inaccuracies of digitizing the published spectra and the absence of any smoothing. Later, in discussing the extrapolation of LEED results to a clean surface value, it is shown that the surface structure results of Jensen *et al.* are compatible with other experiments taking into account estimated surface contamination and error estimates for the structure determination.

The SATLEED code³⁶ of Barbieri and VanHove was used to numerically simulate the I - V spectra. A typical example is shown in Fig. 1 with a corresponding data set. The calculations were based on 13 relativistic phase shifts, which were also calculated using the code of Barbieri and VanHove. Convergence tests in which r factors and structure parameters were evaluated as a function of the number of phase shifts used in the calculation revealed no differences for $l_{\max} \geq 6$. Standard r -factor analysis based on Pendry³⁷ (r_p) and Zanazzi and Jona³⁸ (r_{zj}) r factors (also part of the SATLEED code package) was used to optimize structural and nonstructural parameters leading to structure determination based on measured I - V spectra.

The structure search was initiated by setting nonstructural parameters near the optimized values determined by Jensen *et al.*¹⁵ listed in Table II. The imaginary part of the inner potential (inelastic scattering length) V_{im} was allowed to vary as part of the structure search for each data set. The structure search was restricted to multilayer relaxation of surface atoms assumed to be in registry along the (100) surface normal direction. The range of parameter space searched was d_{12} , 1.36–1.67 Å; d_{23} , 1.44–1.59 Å; and d_{34} , 1.50–1.53 Å (bulk value $d_0 = 1.514$ Å). The parameter V_{im} was varied in 1 eV steps from -3 to -9 eV. The number of layers allowed to relax was varied from 1 to 4. Structure determinations were carried out using both “raw” and smoothed experimental I - V spectra. The raw I - V spectra produced slightly different val-

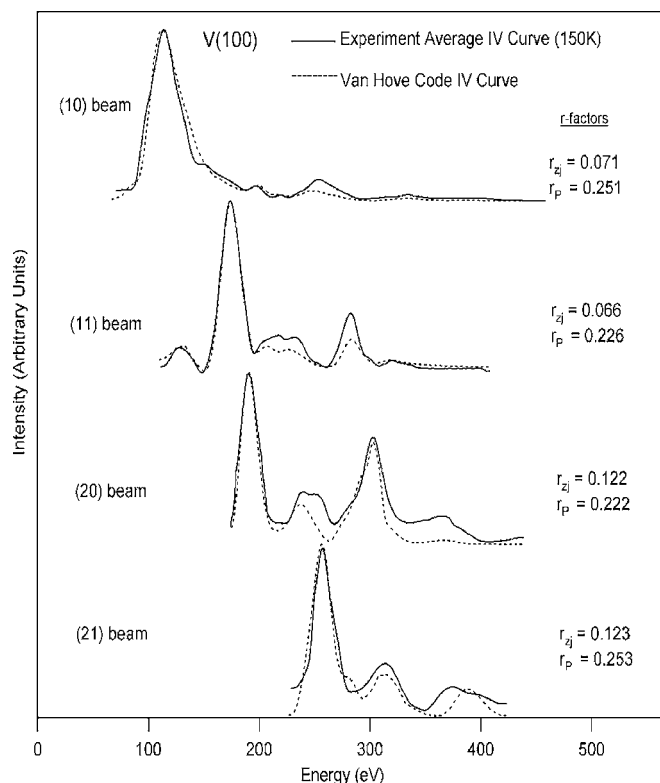


FIG. 1. Representative LEED I - V data set for V(100) plotted with multiple-scattering simulations and r factors characterizing the precision of the experiment and/or calculated fit.

ues for nonstructural parameters and significantly larger r factors than obtained from smoothed data, but the structural results obtained from smoothed and unsmoothed data sets differed very little (Fig. 2). Table II summarizes the set of nonstructural and structural parameters that yielded the best three-parameter fits to 300 and 150 K data sets.

IV. RESULTS FOR SURFACE STRUCTURE

Figure 1 displays experimental I - V spectra (measured at 150 K) along with representative calculated spectra and the accompanying r factors associated with the fit. Table II summarizes the results of several structure searches based on various constraints imposed on structure variations. The total cumulative energy range covered by our V(100) I - V spectra is 1200 eV. The Pendry r factors for our V(100) structure determination exercises are comparable to corresponding values we obtained for W(110) (Ref. 19) (four-beam average $\langle r_p \rangle \sim 0.24$). The Zanazzi-Jona r factors are comparable $\langle r_{zj} \rangle \sim 0.09$ for cumulative energy range of 1200 eV of the W(110) data set. We note that Bergermeyer *et al.*¹³ (Table I) report values of Δ_{12} for V(100) with $r_p = 0.14$ (significantly better than the r_p values obtained in our study). The superior r factor is consistent with the lower concentration of C ($\leq 4\%$) achieved in their clean V(100) surface which leads to lower impurity scattering in the LEED data (that is not accurately modeled in the structure search simulations). The effects of surface contamination on LEED structure determi-

TABLE II. Nonstructural parameters used in multiple-scattering structure searches and Δ_{ij} resulting from three-parameter fit to two LEED data sets. Two-parameter fit results for several data sets are displayed in Fig. 2. Results obtained by Jensen *et al.* are tabulated in right-hand column.

Nonstructural parameters	150 K data set	300 K data set	Jensen <i>et al.</i> (Ref. 15)
Debye temperature (K)	380	380	510
Vibrational constant	1.4	1.4	
Vibrational symmetry	Isotropic	Isotropic	Isotropic
Inner potential (real, eV)	+8.0	+8.0	+9.2
Inner potential (imaginary, eV)	-5.0	-5.0	-4.0
Bulk lattice constant (Å)	1.514	1.514	1.514
Structural parameter ($r_p=0.23$)			
Δ_{12} (%)	-5.4 ± 2.5	-5.4 ± 2.5	-6.7 ± 1.5
Δ_{23} (%)	$+2.5 \pm 2.5$	$+3.4 \pm 2.5$	$+1.0 \pm 1.3$
Δ_{34} (%)	-1.8 ± 1.5	-1.4 ± 1.5	

nation of clean V(100) are discussed in more detail in the following section.

Several data sets were measured and two of the data sets (one at 300 K and one at 150 K) were extensively evaluated based on several assumptions, including constraints on the number of layers allowed to relax, the type of r factor used to determine the best fit, and, in some cases, restricting the analysis to three of the four nondegenerate beam spectra. The

resulting values of d_{12} and d_{23} are presented graphically in Fig. 2. Based on these results, we obtain the following structural parameters for the multilayer relaxation of V(100): $\Delta d_{12} = -5.5\% \pm 1.5\%$, $\Delta d_{23} = +3.39\% \pm 1.5\%$, and $\Delta d_{34} = -1.4\% \pm 1.0\%$ with typical surface C concentration ranging from 5% to 6% during the various measurements. The errors cited represent the convergence precision judged from the scatter of determined structure parameters based on different model constraints and r -factor criteria (Fig. 2). The accuracy of structure determination is discussed in the following section and displayed in Fig. 3 for Δ_{12} as error bars.

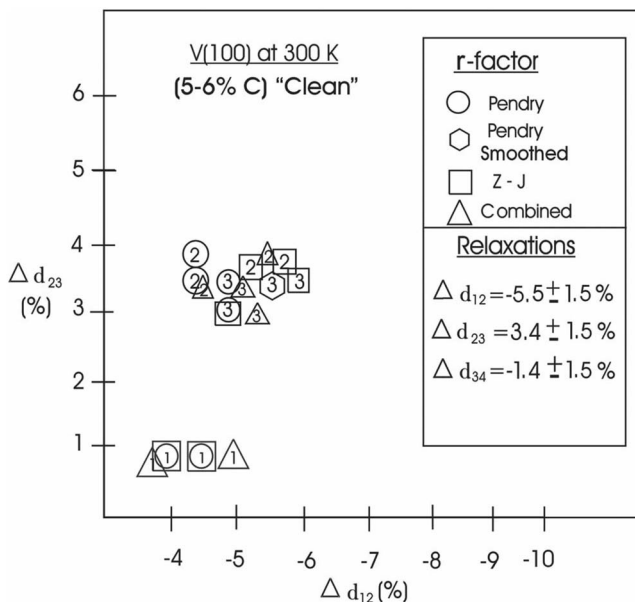


FIG. 2. Graphical representation of variations in determined surface structure resulting from the use of different r factors from using smoothed and unsmoothed experimental 300 K I - V spectra and from using three different models. Number 1 inside a symbol indicates a single-parameter fit (Δ_{12} only allowed to vary with Δ_{23} fixed at +1.0% and other Δ_{ij} held at bulk value) number 2 indicates a two-parameter fit ($\Delta_{12}\Delta_{23}$), and number 3 indicates a three-parameter (Δ_{12} , Δ_{23} , and Δ_{34}) fit. The indicated uncertainties in values of Δ_{ij} in the box reflect the convergence precision of the methodology. The structure accuracy (Table II) is determined by considering the Pendry r factor.

V. SURFACE IMPURITIES AND STRUCTURE ACCURACY

Surface structure and magnetism are both strongly affected by chemisorbed atoms. Therefore, an important factor in using experimental results as a basis for judging the accuracy or validity of an *ab initio* calculation is a realistic assessment of surface impurity concentrations and their effects. The bulk purity of the boule from which a single-crystal sample is prepared can affect the ultimate limit of surface cleanliness achieved in sample preparation. The concentration of bulk carbon in vanadium appears to be the limiting factor in obtaining a clean V(100) surface. In our experiments, the lower limit of surface contamination (after over 1000 h of sputtering and annealing) was 5% C. During LEED and AES experiments in which a tungsten filament was required as an electron source, this concentration would increase to as much as 8% (C+O) after about 1 h. Similar results were reported by Koller *et al.*³¹ Bergermayer *et al.*¹³ reported achieving C impurity levels of 4% in their LEED experiments; Jensen *et al.*¹⁵ reported extensive studies of oxygen contamination in their LEED experiments and stated that C concentrations down to 0.05 ML (5%) were achieved. They also stated that the measured coverage of CO after a set of LEED intensity measurements was below 0.1 ML, but clearly detectable using AES.

Bergermayer *et al.*¹³ carried out extensive experimental [LEED and scanning tunneling microscopy (STM)] and theoretical (*ab initio* calculations) of $c(2 \times 2)$ and $p(2 \times 1)$ car-

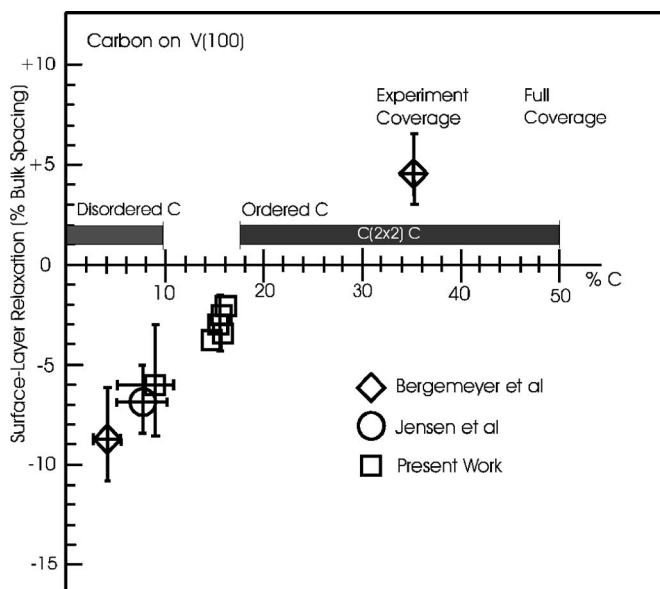


FIG. 3. Values of first-layer relaxation Δ_{12} at V(100) determined by LEED as a function of surface carbon contamination. Carbon concentrations are based uniformly on AES dN/dE calibrations^{13,30} stated in text ($C_{272}/V_{473}=0.10$ for 1 ML carbon), and on AES spectra or surface C concentration stated in the cited papers. Error bars on carbon concentration for present work represents the 5%–8% range of measured C concentrations for all LEED experiments. Error bars on accuracy of Δ_{12} for present work are based on the Pendry r factor (Table II).

bon on V(100). One specific result is an accurate determination of the structure of $c(2 \times 2)$ carbon on V(100). LEED intensity analysis and STM studies establish that $c(2 \times 2)$ C on V(100) occupies the hollow sites, and that at a surface concentration of $\Theta_c \sim 35\%$, that $\Delta_{12} = +4.6\%$. The $c(2 \times 2)$ C structure has been observed down to a surface concentration of 18%; below 10% C, the C layer is disordered and the clean V(100) $p(1 \times 1)$ structure is observed. These results combined with the structure parameters for V(100) from Table I and our additional LEED structure analysis of V(100) surfaces having higher carbon concentrations than 5% yield the results displayed in Fig. 3. This figure illustrates the experimentally determined relationship between Δ_{12} and surface carbon contamination established by LEED crystallography using the previously stated AES calibration criteria. Theoretical models of chemisorption²⁵ (as well as experiments) have shown that surface parameters such as the work function, top-layer relaxation, and the repulsive adsorbate-adsorbate interaction that leads to ordered overlayer structures all of which originate from charge transfer associated with chemisorption, scale linearly with adsorbate concentration for low coverages ($\Theta < 0.1$ ML). It is therefore reasonable to use a linear model to extrapolate measured first-layer relaxation as a function of measured C concentration to the clean surface value. The extrapolation suggests that a realistic clean surface value of d_{12} and Δ_{12} for V(100) to use in judging the validity of an *ab initio* calculation is $d_{12} = 1.36 \pm 0.05 \text{ \AA}$, corresponding to a contraction of $\Delta_{12} \sim 10 \pm 3\%$ relative to the bulk spacing $d_0 = 1.514 \text{ \AA}$. The linear extrapolation appears to extend to the (positive) relax-

ation for $c(2 \times 2)$ C on V(100) at the experimentally determined average surface concentration of $\Theta_c \sim 35\%$ (a coverage significantly beyond the range where a linear extrapolation is expected to be valid).

VI. PROBE FOR SURFACE MAGNETISM AT V(100)

The electron-capture spectroscopy experiment¹⁴ reported in 1986 detected strong spin polarization of V(100) at 300 K that vanished at $T_c = 540$ K. Magnetizing fields along the [001] direction ranging in strength from 103 to 515 Oe were found sufficient to maintain magnetic saturation (no change in detected spin polarization). Surface oxygen contamination of 0.06 ML (6%) at 300 K was found to reduce the spin polarization from 30% to 22%. These experimental results were interpreted as evidence of first-layer long-range ferromagnetic ordering of V(100) with anisotropy energy low enough to be overcome at 300 K by an in-plane applied field of 103 Oe and a Curie temperature $T_c = 540$ K. This result is widely cited in publications dealing with surface magnetism, especially calculations for V(100) (Refs. 8 and 10) surfaces, but has been viewed with skepticism because electron-capture spectroscopy also detected ferromagnetic order in the top layer of $p(1 \times 1)$ V on Ag(100),³⁹ whereas magneto-optic Kerr effect studies²⁷ failed to detect ferromagnetism, and a subsequent *ab initio* calculation⁴⁰ reported that $p(1 \times 1)$ V on Ag(100) is antiferromagnetic.

We have reported prior experimental attempts to detect ferromagnetism in $p(1 \times 1)$ Rh on Ag(100) and $p(1 \times 1)$ V on Ag(100) (Ref. 26) based on the MOKE. The same instrument²⁷ was used to prepare and characterize the clean V(100) surface and carry out an *in situ* probe for magnetism using the MOKE. The sensitivity of the polarimeter has been improved by replacing the He-Ne laser with a solid-state laser. The sensitivity limit achieved in our experiment is discussed below in relation to the expected magneto-optic effects from a magnetic V(100) surface based on layer-dependent magnetic moments predicted by *ab initio* calculations.⁸

Prior experiments on epitaxial Fe on Ag(100),⁴¹ where the Fe magnetic moment $\mu \cong 2.2 \mu_B/\text{atom}$, have shown that typical MOKE rotations and ellipticities of ultrathin films and superlattices are proportional to the film thickness and magnetization and are of the order of 0.007 mrad/ML. In a prior experiment,²⁶ it was shown that a hysteresis loop produced by a 2 ML Fe film on Ag(100) can be integrated to a signal-to-noise ratio of over 100:1 in approximately 100 s, corresponding to a polarimeter sensitivity of $\sim 0.1 \mu\text{rad}$ and a magnetic moment detection sensitivity of less than $0.2 \mu_B/\text{surface atom}$.

The polarimeter calibration experiment, displayed in Fig. 4, demonstrates higher sensitivity. The sensitivity was determined by placing a Faraday cell in the optical path between the polarizer and the V(100) sample. The cell consisted of a 1-mm-thick glass slide (Verdet constant $V \cong 15 \times 10^{-3} \text{ min/Oe cm}$) and a current-carrying coil having its axis along the optical path. This Faraday cell produced rotations of approximately $0.50 \mu\text{rad/Oe}$. The optical quality of the polished bulk crystal V(100) surface after *in situ* cleaning is not quite

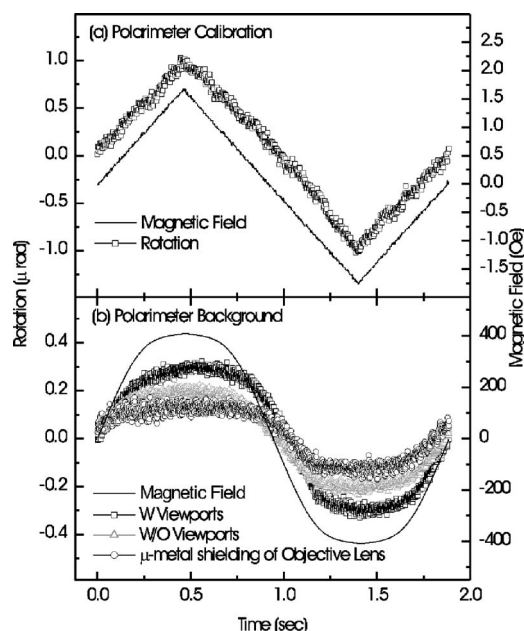


FIG. 4. Upper panel, sensitivity evaluation, and calibration of polarimeter based on Faraday cell showing detected rotation of $1 \mu\text{rad}$ (from triangle wave applied field) with sensitivity corresponding to a signal-to-noise ratio of 20:1. Lower panel; evaluation of background detected signals from stray fields interacting with viewports and optics. The V(100) crystal is replaced by a (nonmagnetic) gold mirror.

equivalent to that of a commercially prepared growth substrate (silicon or sapphire, for example), and some loss in polarimeter sensitivity resulting from light-scattering and depolarization effects is expected. Replacement of the 3 mW He-Ne laser used in prior experiments by a 30 mW solid-state laser has compensated for the reduction in sensitivity associated with the less than ideal optical quality of the bulk V(100) surface. The overall sensitivity of the polarimeter is estimated to be a factor of 4 better than the prior reported value obtained using films on high-quality optical substrates and slightly better than achieved in the study of V and Rh films grown on Ag(100). After 100 s of integration, $\pm 1.0 \mu\text{rad}$ rotation can be measured to a signal-to-noise ratio exceeding 10:1. (corresponding to a sensitivity exceeding $0.05 \mu\text{rad}$).

An estimate of the expected Kerr signal can be obtained from the *ab initio* calculations of the layer-dependent magnetic moment at V(100).⁸ In the favorable case (surface relaxation of $\sim 6\%$ corresponding to the measured values at typical C concentrations in our LEED experiments), the first-layer magnetic moment in units of Bohr magnetons is $+1.452$, with subsequent layer moments of -0.698 , -0.352 , and -0.149 . The net calculated moment for the top four layers is $0.253 \mu_B$. A more elaborate (but not necessarily better) estimate that includes effects of optical penetration $\delta \sim 200 \text{ \AA}$ and assumes that the moments in surface layers after $n=4$ continue the trend of the second, third, and fourth layers (reduction of each following layer moment by factor of 2) yields a net moment of $\mu_{\text{net}}=0.194 \mu_B$. It is reasonable to assume for magnetic V(100) that the MOKE signal will be equivalent to that produced by a 1 ML ferromagnetic film

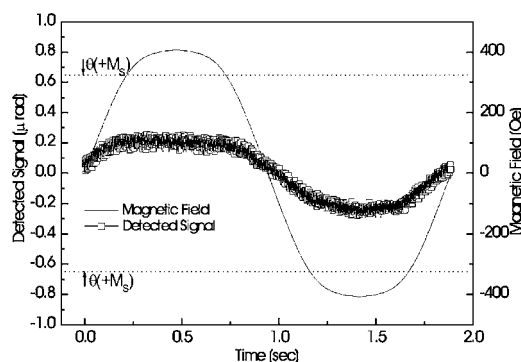


FIG. 5. Detected signal with 400 Oe peak-to-peak magnetic field applied to V(100). Systematic checks (refers to text and Fig. 4) show that the signal is produced by stray fields from the electromagnet that produce Faraday rotation in the vacuum viewports. Any signal produced by the V(100) surface is below the detection limit ($\Theta < 0.05 \mu\text{rad}$). Dotted lines show amplitude of signal based on *ab initio* calculations (refer to text).

having a magnetic moment of $0.2 \mu_B$ (corresponding to a MOKE rotation of $0.65 \mu\text{rad}$). This assumption is strengthened by the fact that *ab initio* calculations^{8,10} attribute a significant fraction of the net V(100) surface magnetic moment to a surface state. Other factors, including spin-orbit coupling strength and optical matrix element weight at the laser wavelength, are assumed equivalent to other metallic ferromagnets (i.e., Fe), which appears to be reasonable.

Surface magnetism at V(100) was probed using the MOKE technique to an estimated sensitivity exceeding $0.05 \mu_B/\text{atom}$, as described in Fig. 4. These conditions require integration of the detected MOKE signal to an equivalent Kerr rotation of less than $0.05 \mu\text{rad}$ at a S/N ratio of 1:1. At this sensitivity, the Faraday rotation produced by the stray-field component of the electromagnet (along the beam axis) interacting with vacuum view ports was easily observed. Consistency tests verified that the detected signal from V(100) (Fig. 5) in phase with the drive field was proportional to the stray magnetic field and was associated with the optical viewports not with the V(100) surface. The range of parameters (applied field of 450 Oe, temperature of 150–300 K, and surface contamination of $< 0.05 \text{ ML O and C}$) covered the range of parameters reported in the electron-capture-spectroscopy experiment.¹⁴ Our MOKE experiments failed to detect evidence of a ferromagnetic V(100) surface at the sensitivity limit of $0.05 \mu_B/\text{surface atom}$.

VII. SUMMARY AND CONCLUSIONS

Experiments that probe the surface structure and search for surface magnetism at V(100) are described. The results are discussed in relation to experimental limitations of preparing a perfectly clean surface and in relation to density-functional calculations. Bulk carbon in V appears to restrict surface sensitive experiments on V(100) to a practical lower limit of 4%–5% carbon concentration. LEED intensity measurements on V(100) with calibrated C surface concentrations below 10% combined with existing published LEED results are used to obtain a meaningful extrapolation of first-

layer relaxation of V(100) to a clean surface value $d_{12} = 1.36 \pm 0.05 \text{ \AA}$ corresponding to a contraction of $10\% \pm 3$ relative to the bulk lattice spacing. A high-sensitivity probe for surface magnetism on technically clean ($C < 5\%$) V(100) failed to detect any evidence of surface magnetism at V(100). The sensitivity of the experiment is estimated to be $0.05 \mu_B/\text{surface atom}$, and the experiment covers the parameter space described in the prior electron-capture spectroscopy experiment¹⁴ that reported ferromagnetic order. It is important to note that the MOKE probes the net magnetic moment averaged over the optical penetration depth (a few hundred angstroms), whereas electron-capture is sensitive only to the surface magnetic moment, and particularly sensitive to a magnetic surface state. In principle, the electron-capture experiment is more sensitive to surface magnetism and represents a more direct probe in the sense that spin polarization is measured. MOKE rotations are indirectly related to spin polarization through spin-orbit coupling and

optical matrix element strengths. Nevertheless, the sensitivity ($0.05 \mu_B/\text{atom}$) of our probe for magnetic order at V(100) should be considered a valid indication that the surface of V(100) is not ferromagnetic.

In relation to the large number of results from *ab initio* calculations for V(100), it is clear that our extrapolated experimental value of top-layer relaxation (to a clean surface value $\Delta_{12} \sim -10\%$) is in good agreement with the typical calculated values. The absence of (or very small) surface magnetic moment at V(100) favors all-electron approaches over pseudopotential approaches in computing magnetic behavior based on *ab initio* methods.

ACKNOWLEDGMENTS

The authors thank Len Kleinman for informative discussions. This work was supported by the Robert A. Welch Foundation (F-1015).

-
- ¹T. G. Walker and H. Hopster, Phys. Rev. B **49**, 7687 (1994).
²P. Fuchs, K. Totland, and M. Landolt, Phys. Rev. B **53**, 9123 (1996).
³M. Finazzia, P. Bencok, H. Hricovini, F. Yubero, F. Chevrier, E. Kolb, G. Krill, M. Vesely, C. Chappert, and J.-P. Renard, Thin Solid Films **317**, 314 (1998).
⁴G. R. Harp, S. S. P. Parkin, W. L. O'Brien, and B. P. Tonner, Phys. Rev. B **51**, 3293 (1995).
⁵M. M. Schwickert, R. Coehoorn, M. A. Tomaz, E. Mayo, D. Lederman, W. L. O'Brien, T. Lin, and G. R. Harp, Phys. Rev. B **57**, 13681 (1998).
⁶I. Turek, S. Blügel, and J. Kudrnovsky, Phys. Rev. B **57**, R11065 (1998).
⁷S. Ohnishi, C. L. Fu, and A. J. Freeman, J. Magn. Magn. Mater. **50**, 161 (1985).
⁸I. G. Batyrev, J.-H. Cho, and L. Kleinman, Phys. Rev. B **63**, 172420 (2001).
⁹G. Bihlmayer, T. Asada, and S. Blügel, Phys. Rev. B **62**, R11937 (2000).
¹⁰T. Bryk, D. M. Bylander, and L. Kleinman, Phys. Rev. B **61**, R3780 (2000).
¹¹R. Robles, J. Izquierdo, A. Vega, and L. C. Balbas, Phys. Rev. B **63**, 172406 (2001).
¹²M. M. J. Bischoff, C. Konvicka, A. J. Quinn, M. Schmid, J. Redinger, R. Podloucky, P. Varga, and H. van Kempen, Phys. Rev. Lett. **86**, 2396 (2001).
¹³W. Bergermayer, R. Koller, C. Knovicka, M. Schmid, G. Kresse, J. Redinger, P. Varga, and P. Podloucky, Surf. Sci. **497**, 294 (2002).
¹⁴C. Rau, C. Liu, A. Schmalzbauer, and G. Xing, Phys. Rev. Lett. **57**, 2311 (1986).
¹⁵V. Jensen, J. N. Anderson, H. B. Nielson, and D. L. Adams, Surf. Sci. **116**, 66 (1982).
¹⁶P. J. Feibelman, Surf. Sci. **360**, 297 (1996).
¹⁷P. J. Feibelman, Phys. Rev. B **53**, 13740 (1996).
¹⁸G. Teeter, D. Hinson, J. L. Erskine, C. B. Duke, and A. Paton, Phys. Rev. B **57**, 4073 (1998).
¹⁹G. Teeter, J. L. Erskine, F. Shi, and M. A. Van Hove, Phys. Rev. B **60**, 1975 (1999).
²⁰G. Teeter and J. L. Erskine, Phys. Rev. B **61**, 13929 (2000).
²¹G. Teeter and J. L. Erskine, Surf. Rev. Lett. **6**, 813 (1999).
²²An earlier test of the consistencies of LEED multiple scattering codes was reported by H.-D. Shih, *Determination of Surface Structures by LEED*, edited by P. M. Marcus and F. Jona (Plenum, New York, 1981).
²³F. Jona, Surf. Sci. **192**, A569 (1987).
²⁴P. M. Marcus, P. Jiang, and F. Jona, Surf. Sci. **192**, A569 (1987).
²⁵M. Scheffler and C. Stampfl, in *Handbook of Surface Science*, edited by K. Horn and M. Scheffler (Elsevier, Amsterdam, 1999), Vol. 2.
²⁶R. L. Fink, C. A. Ballentine, J. L. Erskine, and J. A. Araya-Pochet, Phys. Rev. B **41**, 10175 (1990).
²⁷C. A. Ballentine, R. L. Fink, J. Araya-Pochet, and J. L. Erskine, Appl. Phys. A: Solids Surf. **49**, 459 (1989).
²⁸P. W. Davies and R. M. Lambert, Surf. Sci. **107**, 391 (1981).
²⁹J. S. Foord, A. P. C. Reed, and R. M. Lambert, Surf. Sci. **129**, 79 (1983).
³⁰M. Beutl, J. Lesnik, E. Lundgren, C. Konvicka, P. Varga, and K. D. Rendulic, Surf. Sci. **447**, 245 (2000).
³¹R. Koller, W. Bergermayer, G. Kresse, E. L. D. Hebenstreit, C. Konvicka, M. Schmid, R. Podloucky, and P. Varga, Surf. Sci. **480**, 11 (2001).
³²F. Dulot, P. Turban, B. Kierren, J. Eugène, M. Alnot, and S. Andrieu, Surf. Sci. **473**, 172 (2001).
³³M. Kralj, P. Pervan, M. Milun, K. Wandelt, D. Mandrino, and M. Jenko, Surf. Sci. **526**, 166 (2003).
³⁴G. Krenn, C. Eibl, W. Mauritsch, E. L. D. Hebenstreit, P. Varga, and A. Winkler, Surf. Sci. **445**, 343 (2000).
³⁵Jean Laugier and Bernard Bochu, ORIENTEXPRESS, ENSP/Laboratoire des Matériaux et du Génie Physique, BP 46, 38042 Saint Martin d'Heres, France (<http://www.inpg.fr/LMGP> and <http://www.ccp14.ac.uk/tutorial/lmg>).
³⁶A. Barbieri and M. A. VanHove, AUTOMATED TENSOR LEED Program, Lawrence Berkeley Laboratory.

- ³⁷J. B. Pendry, *J. Phys. C* **13**, 937 (1980).
- ³⁸E. Zanazzi and F. Jona, *Surf. Sci.* **62**, 61 (1977).
- ³⁹C. Rau, G. Xing, and M. Robert, *J. Vac. Sci. Technol. A* **6**, 579 (1988).
- ⁴⁰S. Blügel, D. Drittler, R. Zeller, and P. H. Dederichs, *Appl. Phys. A: Solids Surf.* **49**, 547 (1989).
- ⁴¹S. D. Bader and J. L. Erskine, in *Magnetism in Ultrathin Films*, edited by B. Henrich and J. A. C. Bland (Springer-Verlag, Berlin, 1994), p. 297.